

**NASA
Technical
Paper
2006**

April 1982

Surface Chemistry, Microstructure, and Friction Properties of Some Ferrous-Base Metallic Glasses at Temperatures to 750° C

Kazuhisa Miyoshi and
Donald H. Buckley

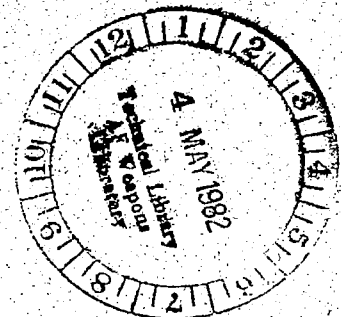
NASA
TP
2006
c.1



TECH LIBRARY KAFB, NM

LOAN COPY: RETURN TO
AFWL TECHNICAL LIBRARY
KIRTLAND AFB, N. M.

NASA



**NASA
Technical
Paper
2006**

1982

TECH LIBRARY KAFB, NM



0067779

Surface Chemistry, Microstructure, and Friction Properties of Some Ferrous-Base Metallic Glasses at Temperatures to 750° C

Kazuhisa Miyoshi and
Donald H. Buckley
*Lewis Research Center
Cleveland, Ohio*

NASA

National Aeronautics
and Space Administration

Scientific and Technical
Information Branch



Summary

X-ray photoelectron spectroscopy (XPS) analysis, transmission electron microscopy, diffraction studies, and sliding friction experiments were conducted to determine the surface chemistry, microstructures, and friction properties of ferrous-base metallic glasses at temperatures to 750° C. Sliding friction experiments were conducted in ultrahigh vacuum with three ferrous-base metallic glasses in contact with an aluminum oxide rider at temperatures to 750° C.

The results of the investigation indicate that the relative concentrations of the various constituents at the surface of the sputtered specimens were very different from the normal bulk compositions. Contaminants can come from the bulk of the material to the surface upon heating and impart boric oxide and silicon oxide at 350° C and boron nitride above 500° C. The coefficient of friction increased with increasing temperature to 350° C. Above 500° C the coefficient of friction decreased rapidly. The segregation of contaminants may be responsible for the friction behavior.

Introduction

To generate an amorphous (or glassy) metallic alloy structure, the molten alloy is rapidly cooled at 1×10^6 °C/sec to avoid the nucleation and grain growth phase of cooling. A noncrystalline (amorphous) alloy so generated may exhibit the same random atomic arrangement as the molten alloy. There are now well over 200 alloy systems that have been identified as being capable of quenching into the amorphous state (ref. 1). These alloys are referred to as metallic glasses (refs. 2 and 3). These amorphous alloys, or metallic glasses, have some very interesting properties. They are as hard as standard steels, yet unlike silicate glasses they possess substantial plasticity, are among the strongest known engineering materials, and resist the propagation of cracks.

Amorphous metals have several features that make them attractive for tribological applications. These features or properties include great shear strength, impact penetration, corrosion resistance, stiffness, and ductility. However, very little research has been done on the tribological properties of amorphous metallic alloys (refs. 4 and 5). The present authors have studied the friction and surface chemistry of some ferrous-base

metallic glasses (ref. 5). We found that these alloys exhibit a higher coefficient of friction in the crystalline state than they do in the amorphous (glassy) state. Surface segregation of alloying materials such as boric oxide or silicon oxide may play an important role in the tribological properties of the amorphous alloys. The surface segregation, microstructure, and tribological properties of the alloys have not as yet been examined in great enough detail.

The objective of this investigation was therefore to determine the surface chemistry, microstructure, and friction properties of some ferrous base metallic glasses at temperatures from room to 750° C. Single-pass sliding friction experiments were conducted with three ferrous-base metallic glass compositions in vacuum (30 nPa). Aluminum oxide riders were made to slide on the metallic glass surfaces under loads to 0.2 N, at a sliding velocity of 0.05 mm/sec, and at temperatures from room to 750° C.

Aluminum oxide has been considered for use in contact with metals because it has been used in a number of practical devices and it has a much higher strength in compression than metals.

Materials

Three metallic glass foil compositions were examined in this investigation. The compositions and some of their properties are listed in table I. The alloys were foils (0.02 to 0.05 mm thick) used in the cast condition. The riders that were made to slide on the foils were single-crystal aluminum oxide (sapphire spheres). The radius of the sapphire rider was 3.2 mm.

Apparatus

The apparatus used in this investigation (fig. 1) was an ultra-high-vacuum system. A device capable of measuring adhesion, load, and friction was mounted in the vacuum system, which also contained an XPS spectrometer. Figure 1 indicates the major components, including the electron energy analyzer, the X-ray source, and the ion gun used for ion sputter etching. The X-ray source contained a magnesium anode. The specimens were mounted on the end of the specimen probe at an angle of 90° from the analyzer axis. The X-ray source was located at an angle of 79° from the analyzer axis.

TABLE I. - PROPERTIES OF METALLIC GLASSES (REF. 2)

Nominal alloy composition, wt%	Crystallization temperature, °C	Density, g/cm ³	Hardness, GPa	Ultimate tensile strength, GPa	Bend ductility, ϵ
Fe ₆₇ Co ₁₈ B ₁₄ Si ₁	430	7.56	10	1.5	1
Fe ₈₁ B _{13.5} Si _{3.5} C ₂	480	7.3	10.3	.7	9×10^{-3}
Fe ₄₀ Ni ₃₈ Mo ₄ B ₁₈	410	8.02	10.5	1.38	1

^a $\epsilon = t/(d - t)$, where t is ribbon thickness and d is micrometer spacing at bend fracture.

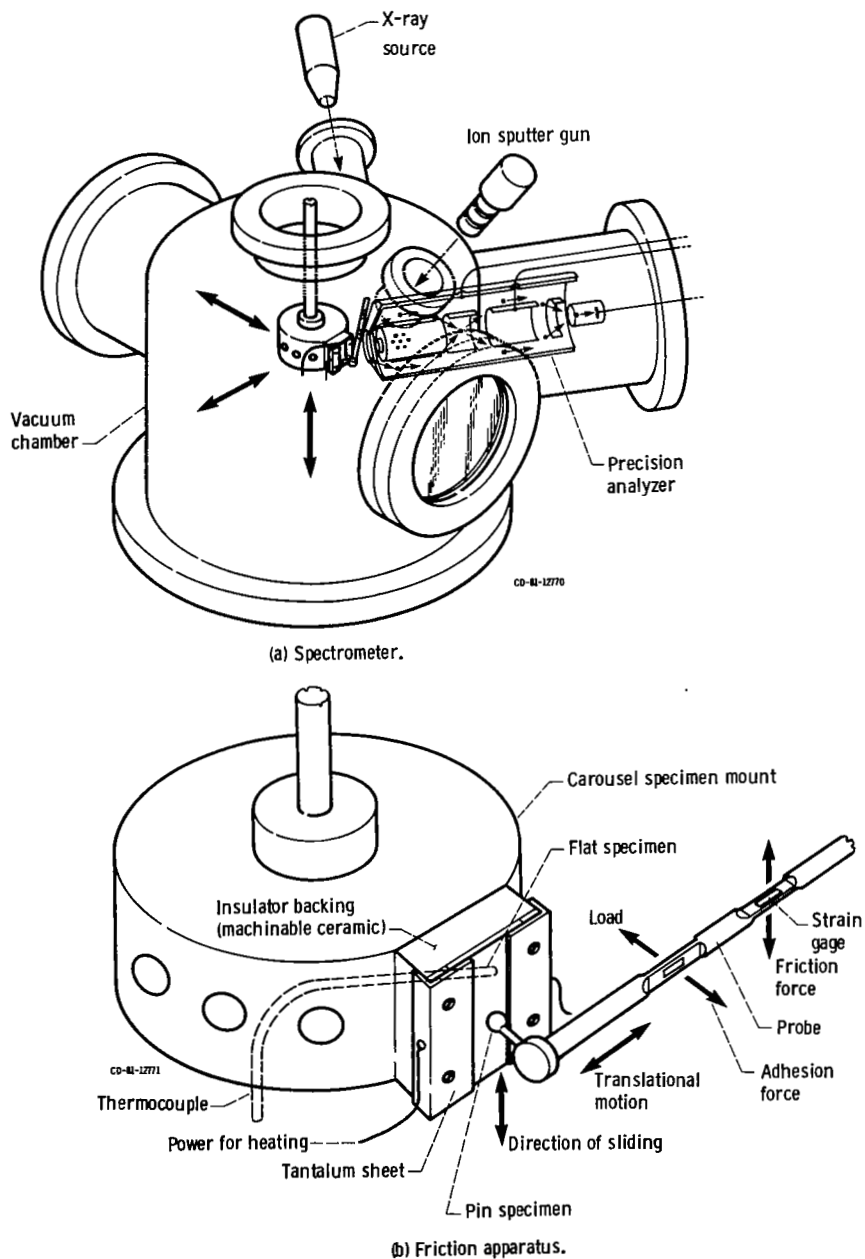


Figure 1. - Schematic representations of the X-ray photoelectron spectrometer and ultra-high-vacuum friction apparatus.

A precision-manipulator-mounted beam was projected into the vacuum chamber. The beam contained two flats machined normal to each other with strain gages mounted thereon. The pin (rider) was mounted on the end of the beam. The load was applied by moving the beam normal to the flat and was sensed by strain gages. The vertical sliding motion of the pin along the flat surface was accomplished through a motorized manipulator assembly. The friction force under an applied load was measured during vertical translation by the strain gage mounted normal to that used to measure load.

Experimental Procedure

Specimen Preparation and Heating

The foil specimen was attached to the insulator flat backing (machinable ceramic) with clamping sheets (fig. 1). The specimen was directly in contact with the sheets. The flat and pin surfaces were rinsed with 200-proof ethyl alcohol just before they were placed in the vacuum chamber. After specimens were placed in the vacuum chamber (fig. 1), the system was evacuated and then baked out at 250° C to obtain a pressure of 30 nPa (2×10^{-10} torr) or lower.

The specimen was heated to 60° C during baking out. Both flat and pin specimens were ion sputter cleaned. Before ion sputter etching, the chamber pressure was 30 nPa or lower, and the ion gun was outgassed for 2 min at a emission current of 20 mA.

The sublimation pump was then flashed on for 2 min at 48 A. The ion pumps were then shut off. The inert gas argon was admitted into the system through a leak valve to the desired pressure, 8 mPa (5×10^{-5} torr). Ion sputter etching was performed with a beam energy equal to 3000 eV at 20-mA emission current with an argon pressure of 8 mPa for the predetermined desired sputter-etching time. The ion beam was continuously rastered over the specimen surface. After sputter etching, the system was reevacuated to a pressure of 30 mPa (2×10^{-5} torr) or lower, and the surface was then examined with the XPS.

Treatment was next conducted in situ on the foil specimen in the vacuum chamber. Treatments included heating to a maximum temperature of 750° C at a pressure of 30 nPa for 20 min and then cooling to room temperature. The foil was also resistance heated to various temperatures for periods of ½ hr at a pressure of 30 nPa. After heating, the specimen was cooled to room temperature. XPS spectra of the foil specimen were obtained before and after heating.

The power for resistance heating the foil specimen was supplied through the tantalum sheets and the foil specimen by a precisely regulated direct-current output

that was adjustable over a wide range. The temperature of the foil specimen was measured with a type K (Alumel-Chromel) thermocouple in direct contact with it.

Specimens were thinned for transmission electron microscopy and diffraction by electropolishing them with a solution of 10 percent perchloric acid in acetic acid.

Chemical Analysis of Surface

The XPS technique is very useful in providing analysis of the first few atomic layers of the specimen surface. The analysis depth with XPS is of the order of 2 to 3 nm, and the ultimate sensitivity is sufficient to allow fractions of a monolayer to be detected and identified.

Both qualitative and quantitative information can be obtained with XPS because all of the elements in the periodic table above helium and its adjacent elements are clearly distinguished. With hydrogen and helium there are not enough occupied energy levels for detection of these elements. The measurements were conducted in the vacuum system (30 nPa).

To obtain reproducible results, a strict standardization of the order and time of recording was used. The instrument was regularly calibrated. The analyzer calibration was determined by using gold as a standard and assuming the binding energy for the gold $4f_{7/2}$ peak to be 83.8 eV; that is, the gold $4f_{7/2}$ level was used as the reference line. All survey spectra, scans of 1050 or 1100 eV, were taken at a pass energy of 50 or 100 eV, thus providing an instrumentation resolution of 1 eV at room temperature. The magnesium $K\alpha$ X-ray source was used with an X-ray source power of 400 W (10 kV, 40 mA). The narrow scans of the C_{1s} , Si_{2p} , and O_{1s} were just wide enough to encompass the peaks of interest and were obtained with a pass energy of 25 eV at room-temperature. Full-width resolution of the spectral peak was 1.5 eV. The energy resolution of the narrow scans was 2 percent of the pass energy, that is, 0.5 eV. The peak maxima could be located to ± 0.1 eV. The reproducibility of the peak height was good, and the probable error in the peak heights ranged from ± 2 percent to ± 8 percent. Peak ratios were generally good to ± 10 percent or less. All XPS analyses were conducted at room temperature.

Friction Experiments

In-situ friction experiments were conducted with the surface-treated foil specimens over a temperature range from room to 750° C. A load of 0.2 N was applied to the pin-flat contact by deflecting the beam, as shown in figure 1. To obtain consistent experimental conditions, contact before sliding was maintained for 30 sec. Both the load and friction force were continuously monitored during a friction experiment. Sliding velocity was 3 mm/min with a total sliding distance of 2 to 3 mm. All

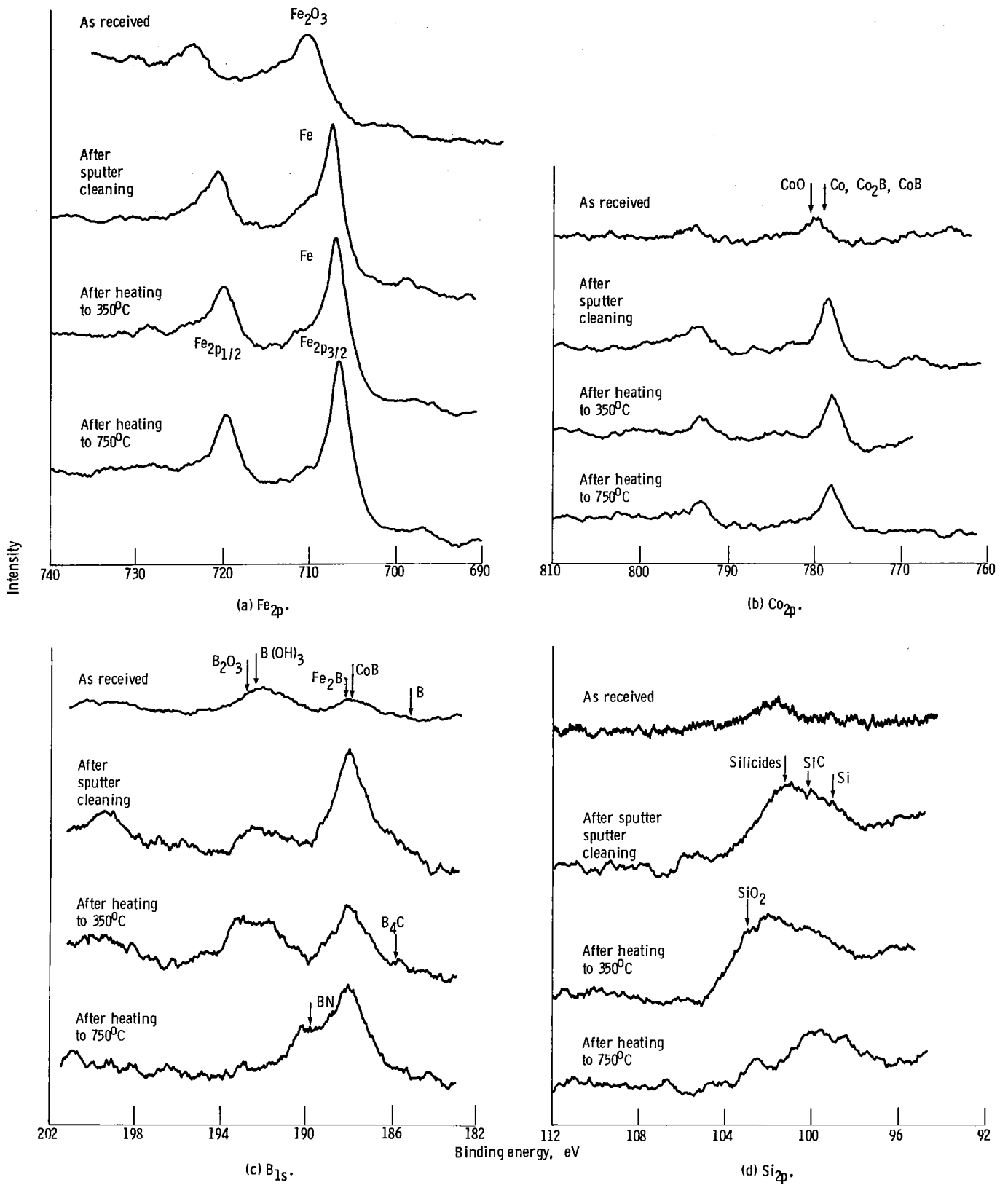


Figure 2. - Representative Fe_{2p} , Co_{2p} , B_{1s} , Si_{2p} , and C_{1s} XPS peaks on $Fe_{67}Co_{18}B_{14}Si_1$ surface.

single-pass friction experiments were conducted in a 30-nPa vacuum. The coefficients of friction reported herein were obtained by averaging three to five measurements. The standard deviations of the data were within ± 4 percent of the average value.

Results and Discussion

Surface Chemistry

Fe₆₇Co₁₈B₁₄Si₁ alloy. – The XPS spectra of the Fe_{2p}, CO_{2p}, B_{1s}, and Si_{2p} obtained from narrow scans on the Fe₆₇Co₁₈B₁₄Si₁ foil surface are presented in figure 2. The as-received foil after bakeout was argon ion bombarded and then heated at various temperatures in a 30-nPa vacuum. All the XPS spectra taken at room temperature reveal carbon and oxygen peaks in addition to iron, cobalt, boron, and silicon.

The Fe_{2p} photoelectron peaks of the as-received specimen clearly indicate that there were iron oxides on the foil surface (ref. 6). The spectra taken after the foil surface had been argon sputter cleaned for 60 min clearly indicate the Fe_{2p} peaks associated with iron, as is typically shown in figure 2. The spectra for the foils heated to 350° and 750° C are almost the same as that for the argon-sputter-cleaned surface.

The CO_{2p} photoelectron peaks of the as-received specimen indicate cobalt oxide at 780 eV. The spectra for the surfaces that had been argon sputter cleaned and heated to 350° and 750° C reveal cobalt and its alloy peaks. The cobalt oxide peak is negligible.

The B_{1s} photoelectron peaks of the as-received specimen indicate the presence of boric oxides as well as Fe₂B, CoB, and B. The spectrum of the surface that had been argon sputter cleaned for 60 min reveals large peaks for boron and its alloys as well as very small boric oxide peaks. The spectra for the foils that had been heated to 350° and 750° C clearly indicate that the foil surfaces were again contaminated with boric oxide and boron nitride that had migrated from the bulk of the foil specimens.

Contaminants such as oxygen, nitrogen, and carbon may be introduced from an environment to the bulk of a metallic glass during the direct casting process. To refine the metallic atomic structure, a metallic glass must be cast at speeds to a few thousand meters per minute and at frequency rates as high as a million degrees centigrade per second.

The Si_{2p} photoelectron peaks of the as-received surface reveal silicides. Even the spectrum of the surface that had been argon sputter cleaned for 60 min reveals silicides as well as silicon oxide on the surface. The foils that had been heated to 350° and 750° C were contaminated with silicon oxide that had migrated from the bulk of the foil specimens.

TABLE II. – COMPOSITION OF METALLIC GLASS SURFICIAL LAYER

[Nominal bulk composition, ^a wt%:
Fe₆₇Co₁₈B₁₄Si₁; nominal bulk
composition, at. %:
Fe₄₂Co₁₁B₄₆Si₁.]

Treatment	Composition on surface, at. %
Argon ion sputtering	Fe ₄₉ Co ₁₄ B ₁₇ Si ₆ C ₉ O ₅
Heating to 350° C	Fe ₅₂ Co ₁₁ B ₁₈ Si ₆ C ₈ O ₅
Heating to 750° C	Fe ₅₄ Co ₉ B ₁₉ Si ₅ C ₈ O ₅

^aManufacturer's analysis.

The composition of the surficial layer of the foil analyzed by XPS is summarized in table II. Generally the XPS results indicate that surfaces that had been cleaned by argon ion sputtering or heated to 350° or 750° C consisted of iron, cobalt, boron, silicon, carbon, and oxygen. The relative concentrations of the constituents on the surfaces were very different from the nominal bulk compositions. The surfaces contained less boron and more silicon, carbon, and oxygen than the bulk.

Fe₈₁B_{13.5}Si_{3.5}C₂ and Fe₄₀Ni₃₈Mo₄B₁₈ alloys. – Generally the surfaces of the as-received, argon-ion-sputter-cleaned, and heated Fe₈₁B_{13.5}Si_{3.5}C₂ and Fe₄₀Ni₃₈Mo₄B₁₈ foils contained carbon and oxygen in addition to the various alloying constituents of the nominal bulk composition. The surface conditions of these foils were basically the same as that for Fe₆₇Co₁₈B₁₄Si₁. The argon-ion-sputter-cleaned surface conditions of the three different foils analyzed by XPS are summarized in table III. The relative concentrations of the various constituents were very different from the nominal compositions. The surfaces contained less boron and more silicon, carbon, and oxygen than the bulk.

Microstructure

To establish the exact crystalline state of the foils examined by XPS as previously described, grain boundary structures were examined by transmission electron microscopy and diffraction in a microscope

TABLE III. – COMPOSITION ON ARGON-SPUTTER-CLEANED SURFACE LAYER OF METALLIC GLASS

Nominal bulk composition		Composition on surface, at. %
wt% ^a	at. %	
Fe ₆₇ Co ₁₈ B ₁₄ Si ₁	Fe ₄₂ Co ₁₁ B ₄₆ Si ₁	Fe ₄₉ Co ₁₄ B ₁₇ Si ₆ C ₉ O ₅
Fe ₈₁ B _{13.5} Si _{3.5} C ₂	Fe ₄₈ B ₄₂ Si ₄ C ₆	Fe ₄₃ B ₁₅ Si ₈ C ₂₁ O ₁₄
Fe ₄₀ Ni ₃₈ Mo ₄ B ₁₈	Fe ₂₃ Ni ₂₁ Mo ₁ B ₅₅	Fe ₁₈ Ni ₂₈ Mo ₁ B ₂₄ C ₁₅ O ₁₄

^aManufacturer's analysis.

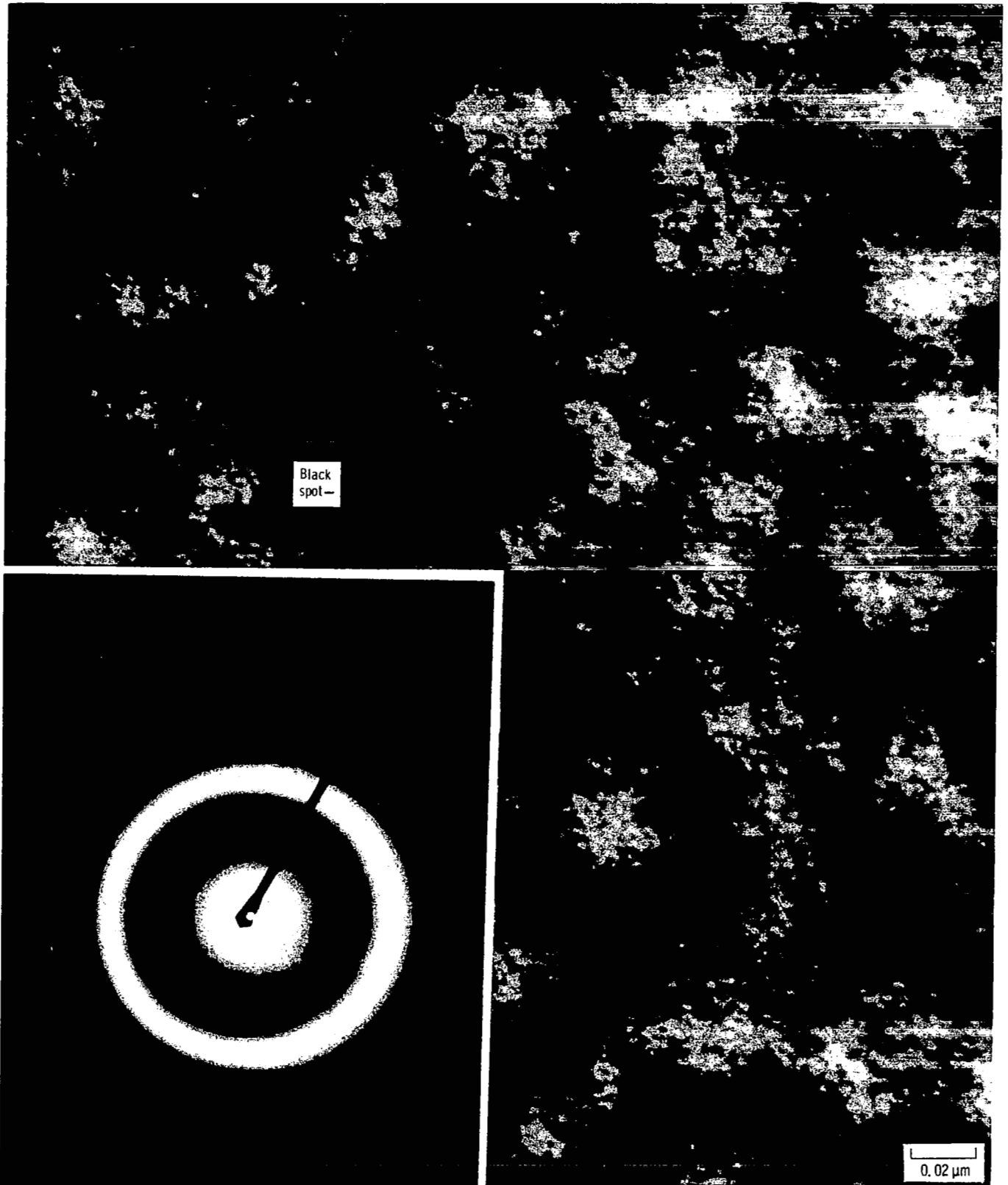


Figure 3. - Typical microstructure and electron diffraction pattern of a metallic glass ($\text{Fe}_{67}\text{Co}_{18}\text{B}_{14}\text{Si}_1$).

operating at 100 kV. Final thinning of the foils was accomplished by electropolishing. These analyses were done after the friction experiments.

A typical example of the structure of the as-received amorphous foil is shown in figure 3. No dislocations or grain boundaries are evident in figure 3. However, black spots, which are believed to be crystallites with a size range from 1.5 to 4 nm, are apparent in the micrograph. The transmission electron diffraction patterns for the as-received foil are also presented in figure 3. The pattern indicates that the amorphous foil was not completely amorphous but contained extremely small grains of approximately a few nanometers in size. Figure 4 presents a typical energy-dispersive X-ray profile of the foil shown in figure 3. The profile shows iron, cobalt, and silicon peaks as well as copper peaks. The copper peaks in the spectrum are associated with the specimen mesh-holder.

A typical example of the crystallized structure of the foil heated to 500° C is shown in figure 5. The foil was subjected to heat treatment above the crystallization temperature in a vacuum of 30 nPa. Complete crystallization occurred after heating to 500° C. The crystallized grain size was about 0.12 to 0.70 μm. At a higher recrystallization temperature of 750° C the recrystallized grain size was 0.3 to 1.4 μm.

Grain boundaries that were not perpendicular to the foil surface contained parallel fringes. Quite frequently regular arrays of twin-like structures were observed within these boundaries, as shown in figures 5 and 6.

A typical microstructure of the foils that had been heated to 500° and 750° C contained two kinds of grains: a dark grain, and a light grain. Single-crystal diffraction patterns were obtained from the dark grain as well as from the light grain after annealing at 750° C, as shown in figure 7. The grains in the foil that had been annealed at 500° C were too small to yield a diffraction pattern. Single-crystal patterns taken from both the dark and light grains included diffraction spots and Kikuchi lines.

Energy-dispersive X-ray analysis was conducted on both dark and light grains. Figure 8 presents a typical

energy-dispersive X-ray profile of the light and dark grains shown in figures 6 and 7. The profile taken from the light grain shows iron, cobalt, and copper peaks but a negligible silicon peak. The copper peaks in the spectrum are associated with the specimen mesh-holder. On the other hand, the spectrum taken from the dark grain clearly shows a silicon peak as well as iron, cobalt, and copper peaks. Thus the segregation of silicon occurs in metallic glasses when they are heated to the recrystallization temperature. No information can be obtained for boron by energy-dispersive X-ray analysis.

Quantitative analysis was done by using X-ray profiles, as shown in figure 8. The relative concentrations of the cobalt and silicon to iron are shown in table IV. Table IV indicates that the dark grains contained much less silicon than the light grains.

Friction Behavior

Sliding friction experiments were conducted with aluminum oxide in contact with metallic glasses in vacuum. Friction-force traces resulting from such sliding are generally characterized by fluctuating behavior with evidence of stick-slip, as is shown in figure 9. All the coefficients of friction reported in figure 10 are defined by $\mu = F/W$, where F is the friction force determined by the average height of the maximum peaks in the friction-force trace and W is the normal load. The coefficient of friction as a function of the sliding temperature of the foil specimen is indicated in figure 10. The aluminum oxide rider was sputter cleaned with argon ions at room temperature. The foil specimen was also sputter cleaned with argon ions in the vacuum system and then heated from room temperature to 750° C. The coefficient of friction increased with increasing temperature from room to 350° C. The increase in friction may be due to an increase in the adhesion resulting from segregation of boric oxide and silicon oxide to the foil surface as shown in figures 2(c) and (d). Above 500° C the coefficient of friction decreased rapidly. The rapid decrease in friction above 500° C correlated with the segregation of boron nitride on the foil surface already discussed and shown in figure 2(c).

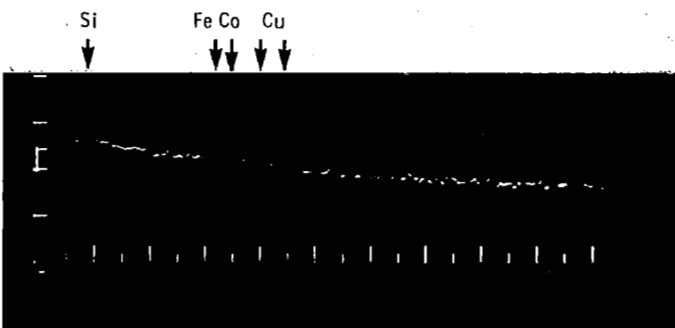


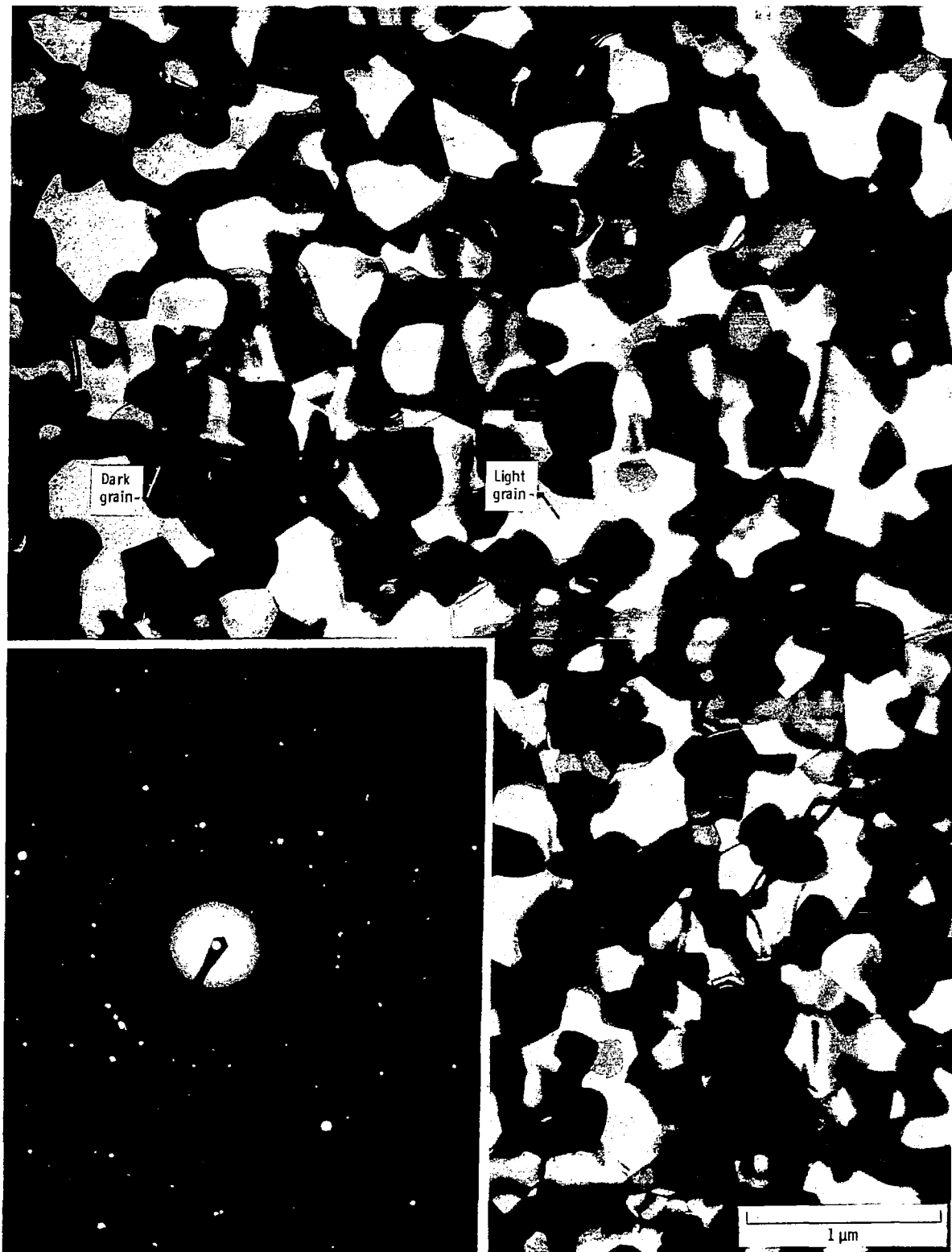
Figure 4. - Energy-dispersive X-ray profile of a metallic glass ($Fe_{67}Co_{18}B_{14}Si_1$).

Conclusions

As a result of XPS analysis, transmission electron microscopy, diffraction studies, and sliding friction experiments conducted with ferrous-base metallic glasses in contact with aluminum oxide in vacuum, the following conclusions were drawn:

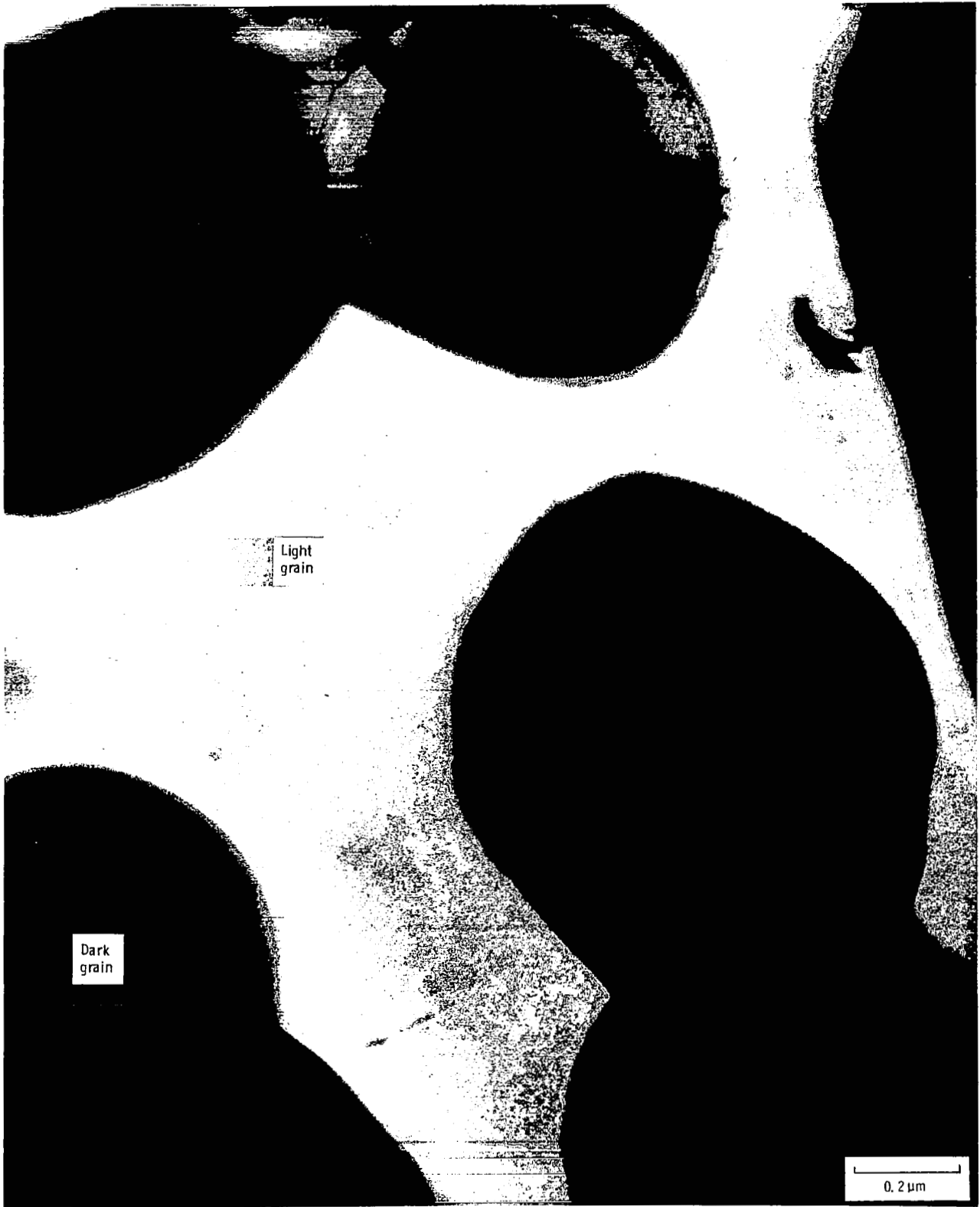
1. The coefficient of friction increases with increasing temperature to 350° C. The increase in friction is believed to be due to an increase in deformation and adhesion





(a) Electron micrograph and diffraction pattern.

Figure 5. - Typical microstructure and electron diffraction pattern of a metallic glass ($\text{Fe}_{67}\text{Co}_{18}\text{B}_{14}\text{Si}_1$) heated to 500°C in vacuum (10 nPa).



(b) High magnification.

Figure 5. - Concluded.

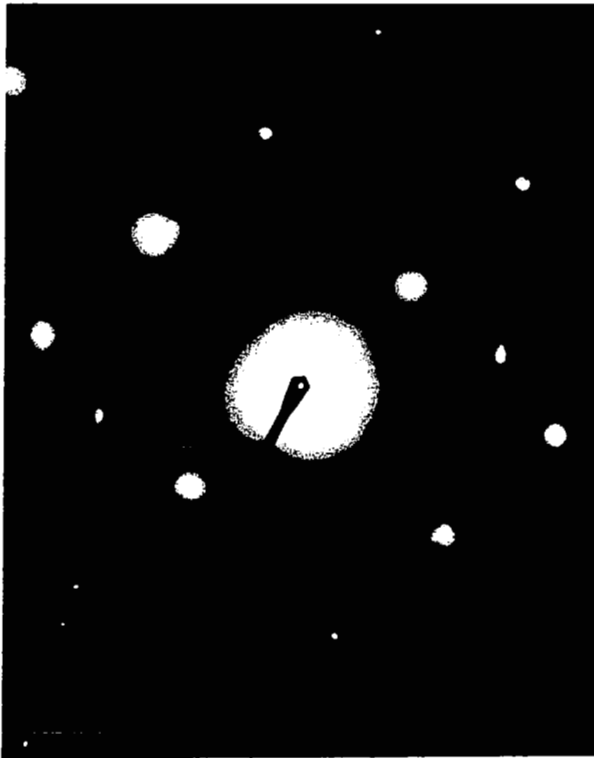




Figure 6. - Typical microstructure of a metallic glass ($\text{Fe}_{67}\text{Co}_{18}\text{B}_{14}\text{Si}_1$) heated to 750°C in vacuum (10 nPa).



Figure 6. - Concluded



(a) Light grain.



(b) Dark grain.

Figure 7. - Electron diffraction patterns taken from the light and dark grains shown in figure 6(b).

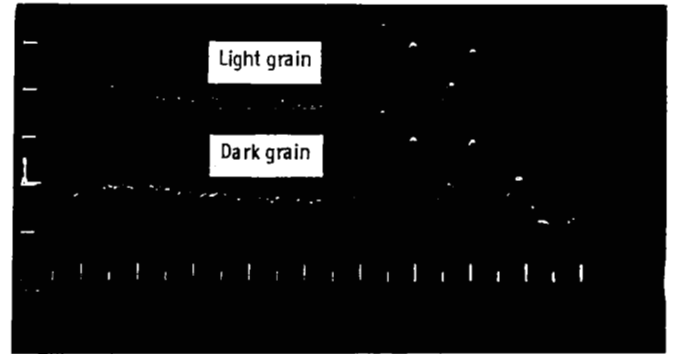


Figure 8. - Energy-dispersive X-ray profile of a metallic glass ($\text{Fe}_{67}\text{Co}_{18}\text{B}_{14}\text{Si}_1$) heated to 750° C in vacuum (10 nPa).

TABLE IV. - SOLUTE-IRON CONCENTRATION RATIO OF BULK OF A METALLIC GLASS HEATED TO 500° OR 750° C IN VACUUM (10 nPa)

(a) Heated to 500° C

Constituent	Structure		
	Dark grain	Light grain	Mixed area
	Solute-iron concentration ratio		
Fe	1	1	1
Co	.3	.44	.36
Si	.001	.02	.008

(b) Heated to 750° C

Fe	1	1	1
Co	.32	.44	.37
Si	.001	.02	.008

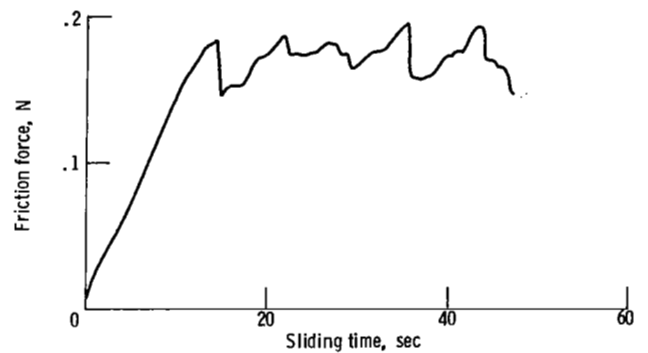


Figure 9. - Typical friction-force trace. Single-pass sliding of 3, 2-mm-rad aluminum oxide rider; sliding velocity, 0.05 mm/sec; load, 0.2 N; room temperature, vacuum pressure, 10 nPa.

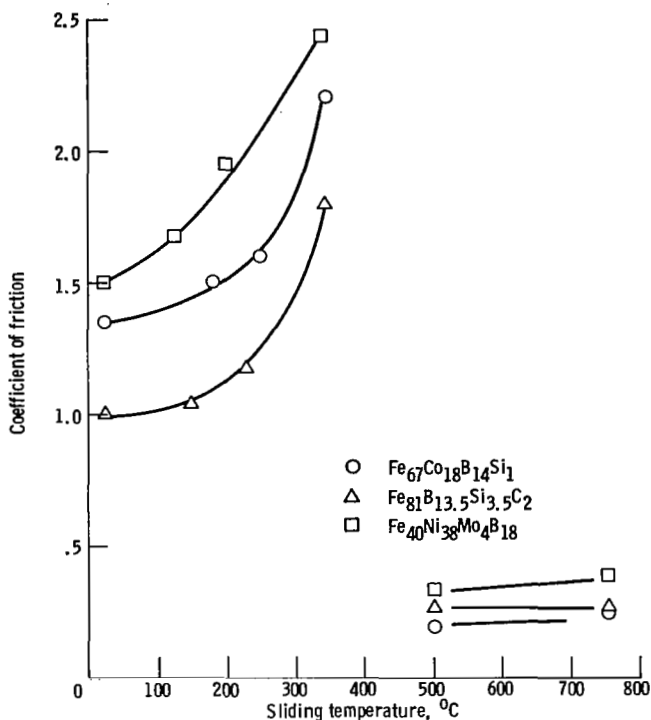


Figure 10. - Coefficient of friction as a function of temperature for aluminum oxide sliding on $\text{Fe}_{67}\text{Co}_{18}\text{B}_{14}\text{Si}_1$, $\text{Fe}_{81}\text{B}_{13.5}\text{Si}_{3.5}\text{C}_2$, and $\text{Fe}_{40}\text{Ni}_{38}\text{Mo}_4\text{B}_{18}$ in vacuum. Normal load, 0.2 N; sliding velocity, 3 mm/min; vacuum, 10 nPa.

resulting from surface segregation of boric oxide and silicon oxide to the surface of the foil.

2. Above 500° C the coefficient of friction decreased rapidly. The decrease may correlate with the segregation of boron nitride to the surface.

3. The physical conclusion to be drawn from surface analysis is that the relative concentrations of the various constituents at the surface of the sputtered specimens are very different from the nominal bulk compositions. The surface generally contains less boron and more carbon and oxygen or silicon than the bulk.

4. Contaminants can come from the bulk of the material to the surface upon heating and impart boric oxide and/or silicon oxide at 350° C and boron nitride above 500° C.

5. The microstructure of crystallized metallic glasses contains dark and light single-crystal grains as revealed by transmission electron microscopy. The dark grains contain considerably less silicon than do the light grains.

Lewis Research Center
National Aeronautics and Space Administration
Cleveland, Ohio, October 30, 1981

References

1. Jones, H.: Splat Cooling and Metastable Phases: Rep. Prog. Phys., vol. 36, 1973, pp. 1425-1497.
2. Gilman, John J.: Metallic Glasses: Phy. Today, vol. 28, no. 5, May 1975, pp. 46-53.
3. Gilman, J. J.: Metallic Glasses—A New Technology. Chapter 111.1, Crystal Growth and Materials, E. Kaldis and H. J. Scheel, eds., North-Holland Publishing Co., 1977, pp. 727-741.
4. Amuzu, J. K. A.: Sliding Friction of Some Metallic Glasses. Journal of Physics D., Applied Physics, vol. 13, no. 7, July 14, 1980, pp. L127-L129.
5. Miyoshi, Kazuhisa; and Buckley, Donald H.: Friction and Surface Chemistry of Some Ferrous-Base Metallic Glasses. NASA TP-1991, 1982.
6. Wagner, C. D.; et al.: Handbook of X-ray Photoelectron Spectroscopy, G. E. Muilenberg, ed., Perkin-Elmer Corp., Physical Electronics Div., Eden Prairie, Minn., 1978.

1. Report No. NASA TP-2006	2. Government Accession No.	3. Recipient's Catalog No.	
4. Title and Subtitle SURFACE CHEMISTRY, MICROSTRUCTURE, AND FRICTION PROPERTIES OF SOME FERROUS-BASE METALLIC GLASSES AT TEMPERATURES TO 750° C		5. Report Date April 1982	
		6. Performing Organization Code 506-53-12	
7. Author(s) Kazuhisa Miyoshi and Donald H. Buckley		8. Performing Organization Report No. E-1001	
		10. Work Unit No.	
9. Performing Organization Name and Address National Aeronautics and Space Administration Lewis Research Center Cleveland, Ohio 44135		11. Contract or Grant No.	
		13. Type of Report and Period Covered Technical Paper	
12. Sponsoring Agency Name and Address National Aeronautics and Space Administration Washington, D. C. 20546		14. Sponsoring Agency Code	
		15. Supplementary Notes	
16. Abstract X-ray photoelectron spectroscopy (XPS) analysis, transmission electron microscopy, diffraction studies, and sliding friction experiments were conducted with ferrous-base metallic glasses in sliding contact with aluminum oxide at temperatures from room to 750° C in a vacuum of 30 nPa. The results indicate that there is a significant temperature influence on the friction properties, surface chemistry, and microstructure of metallic glasses. The relative concentrations of the various constituents at the surface of the sputtered specimens were very different from the normal bulk compositions. Contaminants can come from the bulk of the material to the surface upon heating and impart boric oxide and silicon oxide at 350° C and boron nitride above 500° C. The coefficient of friction increased with increasing temperature to 350° C. Above 500° C the coefficient of friction decreased rapidly. The segregation of contaminants may be responsible for the friction behavior.			
17. Key Words (Suggested by Author(s)) Metallic glasses Microstructure X-ray electron spectroscopy Friction		18. Distribution Statement Unclassified - unlimited STAR Category 26	
19. Security Classif. (of this report) Unclassified	20. Security Classif. (of this page) Unclassified	21. No. of Pages 15	22. Price* A02